

# Scaling of quantum Zeno dynamics in thermodynamic systems

Wing Chi Yu,<sup>1</sup> Li-Gang Wang,<sup>1,2</sup> Shi-Jian Gu,<sup>1,\*</sup> and Hai-Qing Lin<sup>1</sup>

<sup>1</sup>*Department of Physics and ITP, The Chinese University of Hong Kong, Hong Kong, China*

<sup>2</sup>*Department of Physics, Zhejiang University, Hangzhou 310027, China*

(Dated: December 7, 2018)

We study the quantum Zeno effect (QZE) in two many-body systems, namely the one-dimensional transverse-field Ising model and the Lipkin-Meshkov-Glick (LMG) model, coupled to a central qubit. Our result shows that in order to observe QZE in the Ising model, the frequency of the projective measurement should be of comparable order to that of the system sizes. The same criterion also holds in the symmetry broken phase of the LMG model while in the model's polarized phase, the QZE can be easily observed.

PACS numbers: 03.65.Xp, 75.10.Jm

## I. INTRODUCTION

Quantum Zeno effect (QZE) refers to the inhabitation of the unitary time evolution of a quantum system by repeated frequent measurements [1–7]. It is a phenomena which is intrinsically related to the projection postulate in quantum mechanics. For an isolated quantum system, its state vector undergoes an unitary evolution according to the Schrödinger's equation. At the very beginning, the survival probability for the system to remain in the initial state changes quadratically with the elapsed time, while it decreases exponentially in a large time scale. If a measurement is performed to check whether the system is still in the initial state or not after some time, the projection postulate states that the system's state will collapse to the initial state immediately after the measurement. Therefore, when successive measurements are performed at a time interval within the quadratic decaying region, the unitary evolution of the system is found to be suppressed. In the limit of continuous measurement, the dynamic evolution of the system is frozen.

The possibility of such an effect to be found in an unstable quantum system was first pointed out by Fonda *et al.* [11] and Degasperis *et al.* [12]. They suggested that the decay rate of an unstable system may be dependent on the frequency of intermediate measurements. Later, Misra *et al.*, who gave the effect its name, presented a general formulism concerning the semigroups to analyze the QZE [1]. Experimentally, the QZE was first manifested in an radio-frequency transition between two laser-cooled Beryllium ion ground-state levels [13].

In the recent decade, QZE has been studied intensively within the content of quantum optics. Among those analyses, the systems under consideration are only of a few levels in which the QZE can be easily observed by frequent measurements. However, little attention of the possibility to observe QZE in quantum many-body systems has been paid so far. The primary motivation of

our work is to investigate the QZE from the viewpoint of condensed matter physics and obtain criteria on how frequent the measurements should be compared to the system size in order to preserve the QZE in many-body systems.

Mathematically speaking, we are interested in the scaling behavior of the short time limit of the survival probability of the system's initial state under the influence of an external perturbation. We presented a general analysis and find that the leading term of the survival probability is equal to the fluctuation in the interaction Hamiltonian. Specifically, we take the one-dimensional transverse-field Ising model and the Lipkin-Meshkov-Glick (LMG) model as examples. The leading term of the survival probability in these two models are calculated analytically and their scaling behaviors is obtained. In our analysis, we allowed these many-body models to couple to a central qubit. The significance of the central qubit is just to provide an external perturbation in the Hamiltonian and allow us to study how the system's evolution is affected by the external perturbation in the short time regime. A point to note here is that the central qubit only serve as a source of external perturbation and how it evolves is not of our interest. Moreover, we would like to point out that the leading term of the survival probability in our study is just the same as the linear response in the study of quench dynamics [8–10].

The paper is organized as follows: In Section II, we first present a general formulism for obtaining the survival probability of the initial state in the short-time limit. Then in Section III and IV, we take the one-dimensional transverse-field Ising model and the Lipkin-Meshkov-Glick (LMG) model as examples respectively to illustrate the criteria for observing the QZE, in terms of the size dependence of the leading term of the survival probability in the short-time limit. Our analysis shows that in order to observe the QZE, the number of measurements have to be comparable to the size of the system. Finally, a summary would be given in Section V.

---

\*Electronic address: sjgu@phy.cuhk.edu.hk

## II. FORMULISM

Consider a quantum system interacting with the environment, the Hamiltonian of the whole setup can be generally written as

$$H = H_0 + \delta H_I, \quad (1)$$

where  $H_0$  describes the initial Hamiltonian of the system and the environment such that  $H_0|m\rangle = E_m|m\rangle$ . Here  $\{|m\rangle\}$  is a set of orthogonal basis constructed from the tensor product of the eigenstate of the system and that of the environment and  $E_m$  is the corresponding eigenenergy.  $H_I$  is the coupling between the system and the environment with a small parameter  $\delta$  denoting the coupling strength.

Suppose the setup is initially in a state  $|\psi(0)\rangle = |m\rangle$ . It is allowed to evolve freely for a time  $\tau$ . According to the Schrödinger's equation, the state at time  $\tau$  is given by  $|\psi(\tau)\rangle = e^{-iH\tau}|m\rangle$  and the probability of finding the setup in the initial state, i.e. the survival probability, is given by

$$\begin{aligned} P(\tau) &\equiv |p(\tau)|^2 = |\langle\psi(0)|\psi(\tau)\rangle|^2 \\ &= \left| \langle m | e^{-i(H_0 + \delta H_I)\tau} | m \rangle \right|^2. \end{aligned} \quad (2)$$

For small  $\delta$ , one can expand  $p(\tau)$  around  $\delta = 0$  and keep terms up to the second order. We have

$$p(\tau) \approx p(\tau)|_{\delta=0} + \delta \left. \frac{\partial p(\tau)}{\partial \delta} \right|_{\delta=0} + \frac{\delta^2}{2} \left. \frac{\partial^2 p(\tau)}{\partial \delta^2} \right|_{\delta=0}, \quad (3)$$

with

$$\left. \frac{\partial p(\tau)}{\partial \delta} \right|_{\delta=0} = (-i\tau) e^{-i\tau E_m} H_I^{mm}, \quad (4)$$

and

$$\begin{aligned} \left. \frac{\partial^2 p(\tau)}{\partial \delta^2} \right|_{\delta=0} &= -2e^{-i\tau E_m} \\ &\times \sum_{n \neq m} \left[ |H_I^{mn}|^2 \frac{1 - e^{-i\tau(E_n - E_m)} - i\tau(E_n - E_m)}{(E_n - E_m)^2} \right] \\ &- e^{-i\tau E_m} |H_I^{mm}|^2 \tau^2, \end{aligned} \quad (5)$$

where  $H_I^{nm} = \langle n | H_I | m \rangle$ . Keeping terms to the lowest order of  $\delta$ , Eq. (2) becomes

$$P(\tau) \approx 1 - 2\delta^2 \sum_{n \neq m} \frac{1 - \cos[(E_n - E_m)\tau]}{(E_n - E_m)^2} |H_I^{mn}|^2, \quad (6)$$

which is just the perturbative form of the Loschmidt echo [14]. In the short time limit, Eq. (6) gives

$$P(\tau) \approx 1 - \delta^2 \tau^2 \sum_{n \neq m} |H_I^{mn}|^2. \quad (7)$$

Now, suppose successive measurements are performed at every time interval  $\tau$ , and the system is allowed to evolve freely in-between consecutive measurements. The probability of finding the system in the initial state after a finite duration  $\Delta t = Q\tau$ , where  $Q$  is the number of measurements, is

$$P(\Delta t) = |P(\tau)|^Q \approx 1 - \Delta t^2 \delta^2 \frac{\chi}{Q}, \quad (8)$$

where

$$\chi \equiv \sum_{n \neq m} |H_I^{mn}|^2 = \langle m | H_I^2 | m \rangle - \langle m | H_I | m \rangle^2, \quad (9)$$

which is the fluctuation in the interaction Hamiltonian. Note that the projection postulate has been implanted in the first equality in Eq. (8). From Eq. (8), one realized that there exists a competition between  $\chi$  and  $Q$ . For a few-level system, since  $\chi$  is finite, we have  $P(\Delta t) \rightarrow 1$  under the case of continuous measurements ( $Q \rightarrow \infty$ ). In other words, the system would remain in the initial state if the measurements are performed continuously. However, for a quantum many-body system,  $\chi$  may not be finite but goes with some power of the system size. In the thermodynamic limit,  $\chi$  is also infinite and the second term in Eq. (8) could not be simply ignored even if  $Q \rightarrow \infty$ . The key motivation of our work is to obtain the scaling behavior of  $\chi$  in quantum many-body systems. From there, one can then predict the behavior of  $\chi$  in the thermodynamic limit and draw criterions on how large  $Q$  should be in comparison to the system size in order to observe the QZE in the system.

In the following, we take the one-dimensional transverse-field Ising model and the LMG model coupled to a central qubit as examples. Using Eq. (9), we calculated  $\chi$  explicitly and extracted its size dependence. One can then determine the criteria on how large  $Q$  should be in order to observe the QZE in the models.

## III. ONE-DIMENSIONAL TRANSVERSE-FIELD ISING MODEL

The Hamiltonian of the one-dimensional transverse-field Ising model reads

$$H_{\text{Ising}} = - \sum_i (\sigma_i^z \sigma_{i+1}^z + \lambda \sigma_i^x), \quad (10)$$

where  $\sigma_i^q$ , with  $q = x, y, z$ , is the Pauli matrix. It describes a chain of spins interacting with the nearest neighbors in the  $z$  direction, while all the spins are subjected to a transverse external field with strength  $\lambda$  in the  $x$  direction.

The Hamiltonian in Eq. (10) can be diagonalized exactly following three standard transformations [15]: i.e. *Jordan-Wigner transformation*, *Fourier transformation*, and *Bogoliubov transformation*. Then the Hamiltonian in Eq. (10) can be written into an diagonal form of  $H_{\text{Ising}} =$

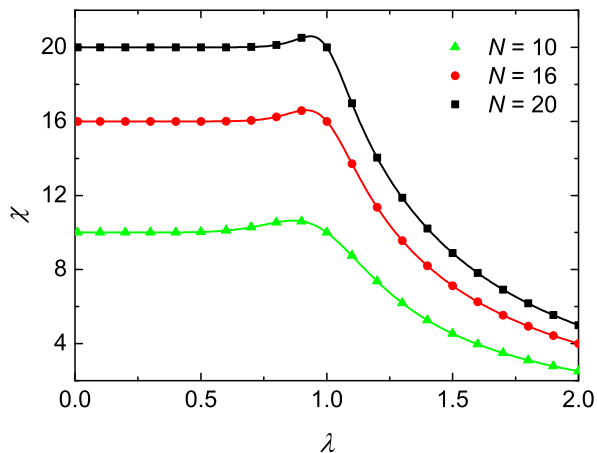


FIG. 1:  $\chi$  as a function of  $\lambda$  for the one-dimensional transverse-field Ising model coupled to a central qubit for system size  $N = 10, 16$  and  $20$ . The symbols denote data obtained from the numerical exact diagonalization while the lines are obtained from the analytical expression of  $\chi$  in Eq. (14). The analytical results agree with the numerical data.

$\sum_k \varepsilon_k (d_k^\dagger d_k - 1/2)$ , where  $\varepsilon_k = 2\sqrt{1 + \lambda^2 - 2\lambda \cos k}$  is the single quasi-particle energy.  $d_k$  and  $d_k^\dagger$  is the fermionic annihilation and creation operator respectively.

Now, consider a central qubit interacting transversely with the Ising model. The corresponding Hamiltonian reads

$$\begin{aligned} H &= H_{\text{Ising}} - \delta \sum_i |e\rangle \langle e| \sigma_i^x, \\ &= H_{\text{Ising}} |g\rangle \langle g| + (H_{\text{Ising}} + \delta H_I) |e\rangle \langle e|, \end{aligned} \quad (11)$$

where  $H_{\text{Ising}}$  is given by Eq. (10), and  $H_I = -\sum_i \sigma_i^x \cdot |g\rangle \langle g|$  and  $|e\rangle$  denotes the ground state and the excited state of the central qubit, respectively. The Loschmidt echo in this system has been investigated by Quan and his collaborators [16]. They found that the decay of Loschmidt echo is greatly enhanced at the critical point of the Ising model. In the following, we will follow similar approach as used by Quan et al., but focusing on the short-time limit of the Loschmidt echo.

Without loss of generality, assume the Ising model is initially in some state  $|\phi(0)\rangle$  and the central qubit is in a superposition state  $c_g |g\rangle + c_e |e\rangle$ , where the coefficients satisfy  $|c_g|^2 + |c_e|^2 = 1$ . The initial state of the whole setup is thus  $|\psi(0)\rangle = |\phi(0)\rangle \otimes (c_g |g\rangle + c_e |e\rangle)$ . The evolution of the Ising chain splits into two branches and the state vector of the setup at a later time  $\tau$  is given by  $|\psi(\tau)\rangle = c_g e^{-iH_{\text{Ising}}\tau} |\phi(0)\rangle \otimes |g\rangle + c_e e^{-i(H_{\text{Ising}} + \delta H_I)\tau} |\phi(0)\rangle \otimes |e\rangle$ .

For simplicity, suppose the Ising chain is initially in the ground state  $|G\rangle$ , and the central qubit is in the excited state, i.e.  $c_g = 0$  and  $c_e = 1$ . The survival probability of the system as given in Eq. (2) becomes

$$P(\tau) = |\langle G| e^{-i(H_{\text{Ising}} + \delta H_I)\tau} |G\rangle|^2. \quad (12)$$

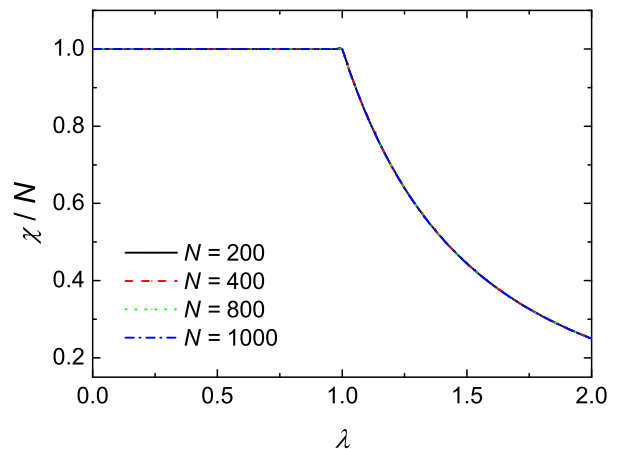


FIG. 2: The normalized  $\chi$  as a function of  $\lambda$  for the one-dimensional transverse-field Ising model coupled to a central qubit. The curve for different system sizes collapses to a single one.

Note that in the eigen-basis of the diagonalized Hamiltonian  $|n_k\rangle$  such that  $d_k^\dagger d_k |n_k\rangle = n_k |n_k\rangle$ , where  $n_k = 0$  or  $1$ , the ground state of the Ising model can be written as  $|G\rangle = \prod_{k>0} |0_k, 0_{-k}\rangle$ .

By performing the Jordan-Wigner transformation, Fourier transformation, and the Bogoliubov transformation,  $H_I$  can also be transformed into the eigen-basis  $\{|n_k\rangle\}$  as

$$\begin{aligned} H_I &= -N \\ &+ \sum_k \left[ 2(\cos \theta_k) d_k^\dagger d_k + i(\sin \theta_k) (d_k^\dagger d_{-k}^\dagger - d_{-k} d_k) \right], \end{aligned} \quad (13)$$

where  $\theta_k$  is the Bogoliubov angle satisfying  $\tan \theta_k = \sin k / (\cos k - \lambda)^{-1}$ . Using Eq. (9), we obtain

$$\chi = \sum_{k>0} \frac{4 \sin^2 k}{1 + \lambda^2 - 2\lambda \cos k}. \quad (14)$$

Next, we would like to investigate the size dependence of  $\chi$ . Assume  $N$  is even, we introduce the density of states in  $k$ -space in the limit of  $N \rightarrow \infty$ . For  $\lambda = 1$ , one gets

$$\chi = \frac{N}{\pi} \int_{\pi/N}^{(N-1)\pi/N} \frac{\sin^2 k}{1 - \cos k} dk \sim N. \quad (15)$$

For  $\lambda \neq 1$ , let  $0 \leq x \leq 1/2$  and  $0 \leq k = 2\pi x \leq \pi$ , then Eq. (14) becomes

$$\chi = 2N \int_0^1 \frac{\sin^2 2\pi x}{1 + \lambda^2 - 2\lambda \cos 2\pi x} dx. \quad (16)$$

Let  $z = e^{i2\pi x}$ , so  $\sin(2\pi x) = \frac{1}{2i}(z - \frac{1}{z})$  and  $\cos(2\pi x) = \frac{1}{2}(z + \frac{1}{z})$ , the integral becomes the contour integral along a unit circle on the complex plane:

$$\chi = \frac{N}{4\pi i} \oint \frac{(z^2 - 1)^2}{z^2(z - \lambda)(\lambda z - 1)} dz, \quad (17)$$

which can be easily evaluated using the residue theorem. One then obtains

$$\chi = \begin{cases} N/\lambda^2 \sim N & \text{for } \lambda > 1 \\ N \sim N & \text{for } \lambda < 1. \end{cases} \quad (18)$$

To check the validity of the result obtained above, one may consider the limiting case where  $\lambda \rightarrow 0$ . In this limit, the ground state of the system is a superposition of two polarized wavefunctions, i.e.  $\frac{1}{\sqrt{2}}(|\uparrow\uparrow\cdots\uparrow\rangle + |\downarrow\downarrow\cdots\downarrow\rangle)$ . Noting that the interaction Hamiltonian  $H_I$  only flips a particular spin at site  $i$ . This results in a wavefunction orthogonal to the original one. The second term in Eq. (9) is thus zero. For the first term, one can also easily verify that gives  $N$  using the property of the Pauli's matrices. Therefore, one obtains  $\chi = N$  as  $\lambda \rightarrow 0$ . On the other hand, from the analytical expression in Eq. (14), we also obtain the same result for  $\lambda = 0$  as shown in Eq. (18).

Furthermore, we also perform the numerical exact diagonalization and calculated  $\chi$  using Eq. (9). Fig. 1 shows a plot of  $\chi$  as a function  $\lambda$  for  $N = 10, 16$  and  $20$ . The lines obtain from the analytical expression of  $\chi$  agree with the numerical data (represented by symbols).

Fig. 2 shows a plot of  $\chi$  given by the analytical expression in Eq. (14) normalized over the system size as a function of  $\lambda$ . The curve for different system sizes collapse to a single one, i.e.  $\chi \sim N$ . This echoes the result obtained from the scaling analysis above.

Returning to Eq. (8), we see that in order to observe QZE in the Ising model,  $Q \gg \xi N$  where  $\xi$  is a constant independent of the system size. In the thermodynamic limit, in which  $N$  is of order  $10^{23}$ ,  $Q$  has to be at least of this order or else the QZE breaks down.

From Fig. 2, one can also realize that the normalized  $\chi$  changes manifestly across the point at  $\lambda = 1$ , which is the critical point where a quantum phase transition (QPT) of the Ising model takes place [15]. Differentiating Eq. (14) with respect to  $\lambda$ , one obtains

$$\frac{d\chi}{d\lambda} = \sum_{k>0} \frac{8(\cos k - \lambda) \sin^2 k}{(1 + \lambda^2 - 2\lambda \cos k)^2}. \quad (19)$$

A plot of Eq. (19) normalized over the system size as a function of  $\lambda$  in the vicinity of the critical point is shown in Fig. 3.  $d(\chi/N)/d\lambda$  changes from positive to negative as the system goes across the critical point from below. This change becomes sharper and sharper as the system size increases. Fig. 4 shows the second derivative of the normalized  $\chi$  as a function of  $\lambda$  in the vicinity of the critical point. One can see that  $d^2(\chi/N)/d\lambda^2$  exhibits a minimum at the critical point. The magnitude of this minimum is in fact scales with  $N$ , as shown in the inset of Fig. 4.

The size dependence of  $d^2(\chi/N)/d\lambda^2$  can also be obtained analytically. Differentiate Eq. (19) with respect

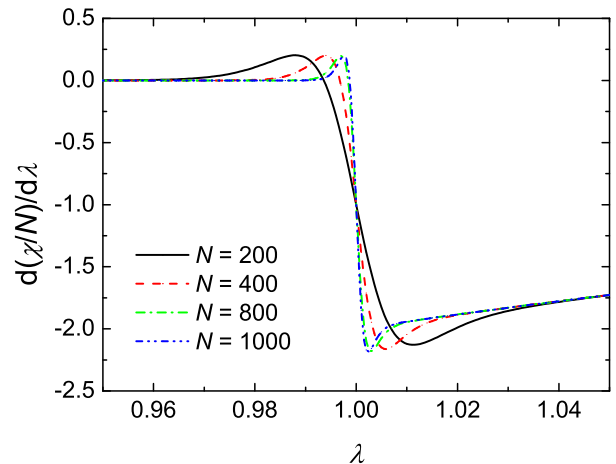


FIG. 3: The first derivative of the normalized  $\chi$  with respect to  $\lambda$  as a function of  $\lambda$  near the vicinity of the critical point for the one-dimensional transverse-field Ising model coupled to a central qubit.  $d(\chi/N)/d\lambda$  changes from positive to negative across the critical point of the Ising model. The change is faster for a larger system size. The curve for different system sizes coincide exactly at  $\lambda = 1$ .

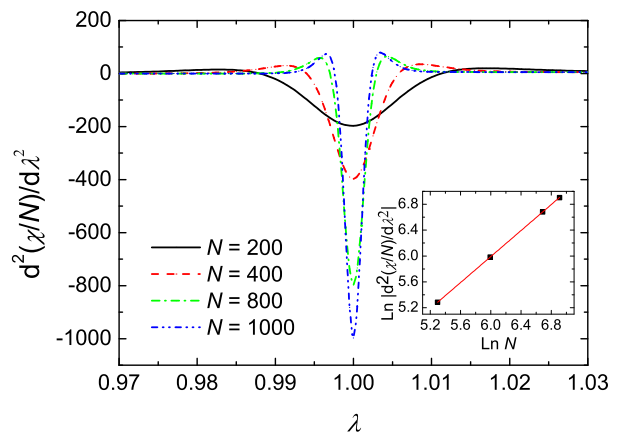


FIG. 4: The second derivative of the normalized  $\chi$  with respect to  $\lambda$  as a function of  $\lambda$  near the vicinity of the critical point for the one-dimensional transverse-field Ising model coupled to a central qubit. The inset shows the scaling behavior of the minimum of  $d^2(\chi/N)/d\lambda^2$ . The slope of the straight line is  $1.007 \pm 0.001$ .

to  $\lambda$ , one obtains

$$\frac{d^2\chi}{d\lambda^2} = \sum_{k>0} \left[ \frac{32(\lambda - \cos k)^2 \sin^2 k}{(1 + \lambda^2 - 2\lambda \cos k)^3} - \frac{8 \sin^2 k}{(1 + \lambda^2 - 2\lambda \cos k)^2} \right]. \quad (20)$$

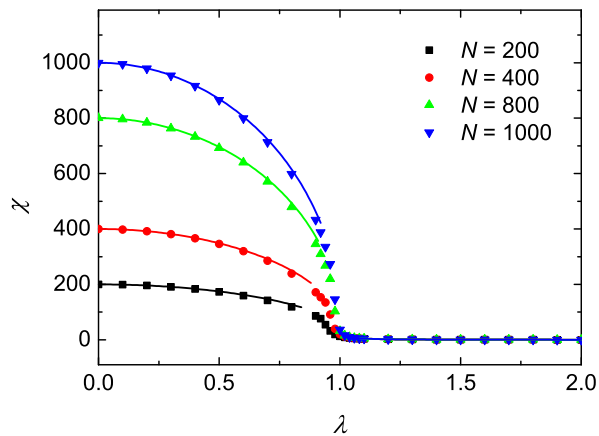


FIG. 5:  $\chi$  as a function of  $\lambda$  for the LMG model coupled to a central qubit with system sizes  $N = 800$  and  $1000$  ( $\gamma = 0$ ). The dots denote data obtained from the numerical exact diagonalization while the smooth lines are obtained from the analytical expression of  $\chi$  in Eq. (38) and (40). The analytical results agree with the numerical data except for points close to  $\lambda = 1$ .

For  $\lambda = 1$ ,

$$\begin{aligned} \frac{d^2\chi}{d\lambda^2} &= \sum_{k>0} \left[ \frac{4 \sin^2 k}{1 - \cos k} - \frac{2 \sin^2 k}{(1 - \cos k)^2} \right], \\ &= \frac{N}{\pi} \int_{\pi/N}^{(N-1)\pi/N} \left[ 2(1 + \cos k) - \frac{1 + \cos k}{1 - \cos k} \right] dk, \\ &\sim N^2. \end{aligned} \quad (21)$$

We then have  $d^2(\chi/N)/d\lambda^2 \sim N$  which diverges in the thermodynamic limit.

Furthermore, from Fig. 3, we see that there exists a fixed point at  $\lambda = 1$  where  $d(\chi/N)/d\lambda$  for various system size coincide. This can also be shown analytically from Eq. (19). For  $\lambda = 1$ , Eq. (19) gives

$$\begin{aligned} \frac{d(\chi)}{d\lambda} &= \sum_{k>0} \frac{2 \sin^2 k}{1 - \cos k} \\ &= \frac{N}{\pi} \int_{\pi/N}^{(N-1)\pi/N} (1 + \cos k) dk \\ &= -N, \end{aligned} \quad (22)$$

in which the average over system size gives  $-1$ . This fixed point reflects some kind of symmetry is hidden in the model and further exploration would be of interest.

#### IV. LIPKIN-MESHKOV-GLICK MODEL

The Hamiltonian of the LMG model reads

$$H_{\text{LMG}} = -\frac{1}{N} \sum_{i<j} (\sigma_i^x \sigma_j^x + \gamma \sigma_i^y \sigma_j^y) - \lambda \sum_i \sigma_i^z. \quad (23)$$

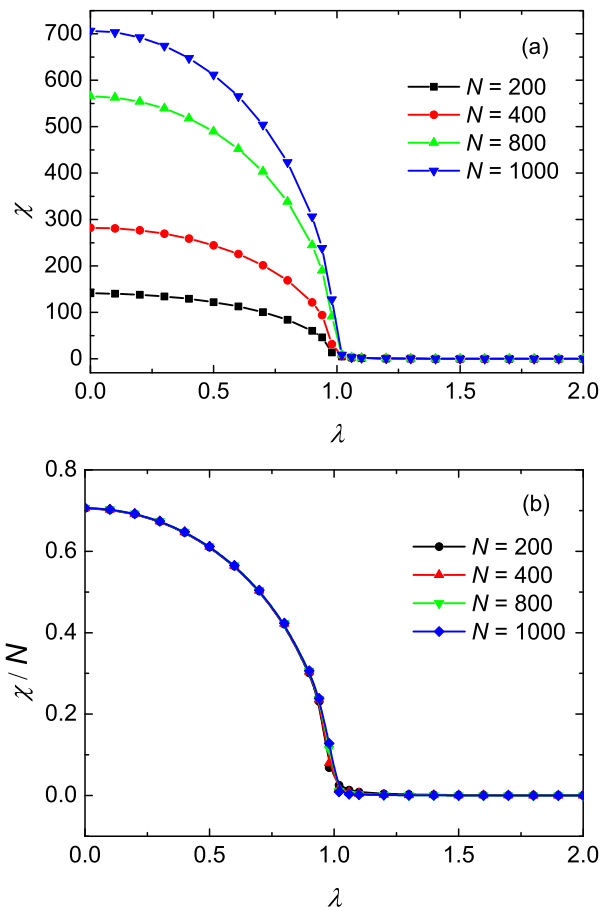


FIG. 6: (a)  $\chi$  as a function of  $\lambda$  (b) The normalized  $\chi$  as a function of  $\lambda$  for different system sizes for the LMG model coupled to a central qubit ( $\gamma = 0.5$ ). The normalized  $\chi$  for various system sizes collapse to a single curve.

The Hamiltonian describes a cluster of spins mutually interacting with each other in the  $xy$  plane.  $\gamma$  is the parameter indicating the anisotropy in the interaction of the model. All the spins are embedded in an external field along the  $z$  direction. The prefactor  $1/N$  is to ensure a finite energy per spin in the thermodynamic limit. Introducing  $S_\kappa = \sum_i \sigma_i^\kappa / 2$ , where  $\kappa = x, y, z$ , and  $S_x = (S_+ + S_-)/2$  and  $S_y = (S_+ - S_-)/2i$ , Eq. (23) can be rewritten as

$$\begin{aligned} H_{\text{LMG}} &= -2\lambda S_z - \frac{1}{2N} (1 - \gamma) (S_+^2 + S_-^2) \\ &\quad - \frac{1}{N} (1 + \gamma) \left( S^2 - S_z^2 - \frac{N}{2} \right). \end{aligned} \quad (24)$$

In the large  $N$  limit and considering the low excitation spectrum, the above Hamiltonian can be diagonalized through a semi-classical approach as in the following[17]:

(i) Perform a rotation of the spin operators around the  $y$  axis in order to bring the  $z$  axis along the semiclassical

magnetization. This is done by

$$\begin{pmatrix} S_x \\ S_y \\ S_z \end{pmatrix} = \begin{pmatrix} \cos \alpha & 0 & \sin \alpha \\ 0 & 1 & 0 \\ -\sin \alpha & 0 & \cos \alpha \end{pmatrix} \begin{pmatrix} \tilde{S}_x \\ \tilde{S}_y \\ \tilde{S}_z \end{pmatrix}, \quad (25)$$

where  $\alpha = 0$  for  $\lambda > 1$  so that  $\mathbf{S} = \tilde{\mathbf{S}}$ , and  $\alpha = \cos^{-1} \lambda$  for  $\lambda < 1$ .

(ii) *Holstein-Primakoff transformation* which transforms the spin operators into bosonic operators by

$$S_z = S - a^\dagger a = N/2 - a^\dagger a, \quad (26)$$

$$S_+ = (2S - a^\dagger a)^{1/2} a = \sqrt{N} (1 - a^\dagger a/N)^{1/2} a, \quad (27)$$

$$S_- = a^\dagger (2S - a^\dagger a)^{1/2} = \sqrt{N} a^\dagger (1 - a^\dagger a/N)^{1/2}, \quad (28)$$

where  $a$  and  $a^\dagger$  are bosonic annihilation and creation operators satisfying the commutation relation  $[a, a^\dagger] = 1$ . The second equality in above equations hold as a result of  $[H, S^2] = 0$  and only the low energy spectrum is considered.

(iii) *Bogoliubov transformation*: After the above transformations, we arrive at a quadratic Hamiltonian and one can easily diagonalize it using the Bogoliubov transformation:

$$a = \sinh\left(\frac{\theta}{2}\right) b^\dagger + \cosh\left(\frac{\theta}{2}\right) b, \quad (29)$$

$$a^\dagger = \cosh\left(\frac{\theta}{2}\right) b^\dagger + \sinh\left(\frac{\theta}{2}\right) b, \quad (30)$$

where  $b$  and  $b^\dagger$  are also bosonic operators satisfying the same commutation relation as that of  $a$  and  $a^\dagger$ . Following the above transformations, one could finally diagonalize the Hamiltonian in Eq. (24) into  $H_{\text{LMG}} = \epsilon_0 N + \epsilon_1 - \Delta/2 + \sqrt{\Delta^2 - 4\Gamma^2} (b^\dagger b + 1/2)$ , where for  $\lambda < 1$ ,

$$\begin{cases} \epsilon_0 = -\frac{1 + \lambda^2}{2} \\ \epsilon_1 = \frac{1 - \lambda^2}{2} \\ \Delta = 2 - \lambda^2 - \gamma \\ \Gamma = \frac{\gamma - \lambda^2}{2} \end{cases}. \quad (31)$$

For  $\lambda > 1$ ,

$$\begin{cases} \epsilon_0 = -\lambda \\ \epsilon_1 = 0 \\ \Delta = 2\lambda - 1 - \gamma \\ \Gamma = -\frac{1 - \gamma}{2} \end{cases}. \quad (32)$$

The diagonalization condition is given by

$$\tanh \theta = -\frac{2\Gamma}{\Delta}, \quad (33)$$

from which we also have

$$\cosh \theta = \frac{\Delta}{\sqrt{\Delta^2 - 4\Gamma^2}}, \quad \sinh \theta = \frac{-2\Gamma}{\sqrt{\Delta^2 - 4\Gamma^2}}. \quad (34)$$

Similar to the case of the Ising model in the previous section, let's consider a central qubit interacting transversely with the LMG model. The corresponding Hamiltonian reads

$$H = H_{\text{LMG}} - \delta \sum_i |e\rangle \langle e| \sigma_i^z, \quad (35)$$

where  $H_{\text{LMG}}$  is given by Eq. (23). Again, suppose the LMG model is initially in the ground state  $|G\rangle$ , and the central qubit is in the excited state. Following the same argument as in the Ising model, the survival probability of the system remain in the initial state in Eq. (2) becomes

$$P(\tau) = |\langle G | e^{-i(H_{\text{LMG}} + \delta H_I)\tau} | G \rangle|^2, \quad (36)$$

where  $H_I = -\sum_i \sigma_i^z$ . Similarly, in the eigen-basis  $\{|n\rangle\}$  such that  $b^\dagger b |n\rangle = n |n\rangle$ , where now  $n = 0, 1, 2, \dots$ , note that ground state of the LMG model is just  $|G\rangle = |0\rangle$ . Following the diagonalization procedure mentioned above,  $H_I$  can also be expressed in the eigen-basis  $\{|n\rangle\}$ . For  $\lambda > 1$ ,

$$H_I = N + 1 - \cosh \theta - 2 \cosh(\theta) b^\dagger b - \sinh(\theta) (b^{\dagger 2} + b^2). \quad (37)$$

Using Eq. (9), (34), and (37), one obtains

$$\chi = 2 \sinh^2 \theta \sim N^0. \quad (38)$$

For  $\lambda < 1$ ,

$$H_I = -\lambda(N - \cosh(\theta) + 1) + 2 \cosh(\theta) b^\dagger b + \lambda \sinh(\theta) (b^{\dagger 2} + b^2) + \sqrt{N(1 - \lambda^2)} (b^\dagger + b) (\cosh(\theta/2) + \sinh(\theta/2)). \quad (39)$$

Using Eq. (9), (34), and (40), one has

$$\begin{aligned} \chi &= 2\lambda \sinh^2 \theta \\ &\quad + \lambda \sqrt{N(1 - \lambda^2)} \sinh \theta (\sqrt{\cosh \theta + 1} + \sqrt{\cosh \theta - 1}) \\ &\quad + (1 - \lambda^2) N (\cosh \theta + \sinh \theta) \\ &\sim N. \end{aligned} \quad (40)$$

Again, to check the validity of the analytical result, let's first consider the limiting case where  $\gamma = 0$  and  $\lambda \rightarrow 0$ . In this limit, the Hamiltonian as given by Eq. (23) is similar to that of the Ising model except the interaction is over all spins here. Following similar argument as that for the Ising model,  $\chi$  obtained from Eq. (9) also gives  $N$ . On the other hand, from Eq. (31) and (34), one can easily see that Eq. (40) also gives  $N$ . The two results are consistent.

Moreover, the analytical result is also compared with the data from the numerical exact diagonalization. As shown in Fig. 5, the two data agree with each other except for  $\lambda$  close to 1. This invalidity of the analytical result for finite system sizes near the critical point is due to the fact that we have only kept terms up to the lowest

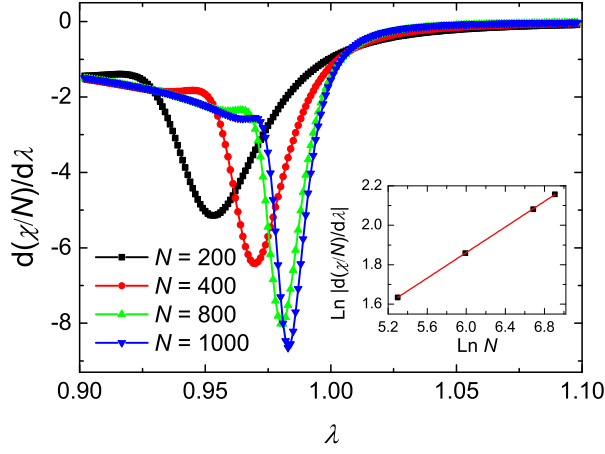


FIG. 7: First derivative of the normalized  $\chi$  with respect to  $\lambda$  as a function of  $\lambda$  in the vicinity of the critical point for the LMG model coupled to a central qubit ( $\gamma = 0.5$ ). The inset shows the scaling behavior of the minimum of  $d(\chi/N)/d\lambda$ . The slope of the straight line gives  $0.324 \pm 0.001$ .

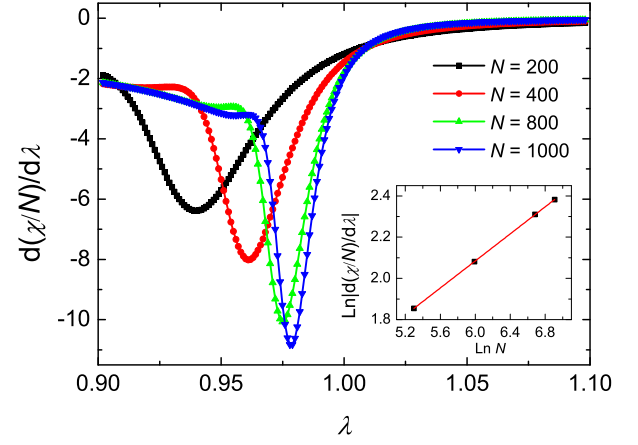


FIG. 9: First derivative of the normalized  $\chi$  with respect to  $\lambda$  as a function of  $\lambda$  in the vicinity of the critical point for the LMG model coupled to a central qubit ( $\gamma = 0$ ). The inset shows the scaling behavior of the minimum of  $d(\chi/N)/d\lambda$ . The slope of the straight line gives  $0.328 \pm 0.001$ .

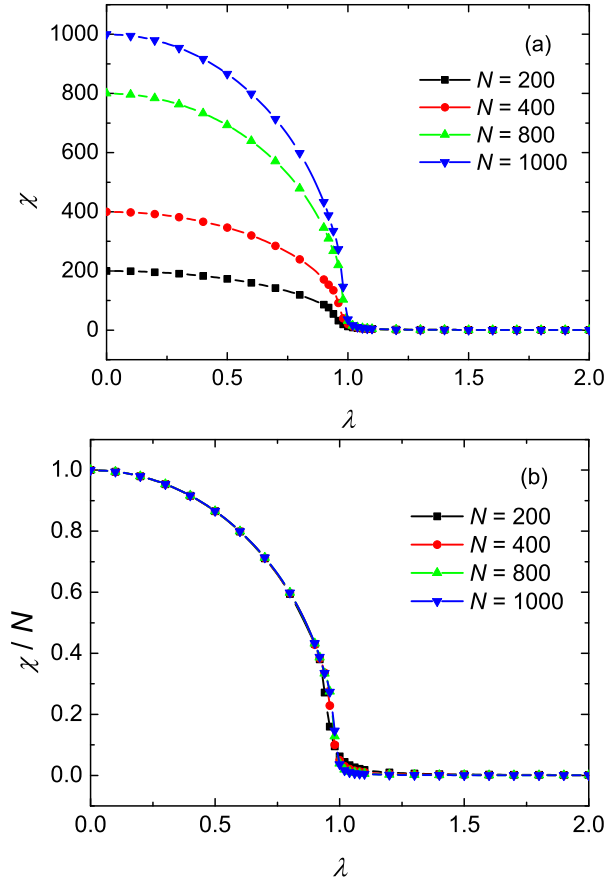


FIG. 8: (a)  $\chi$  (b) The normalized  $\chi$  for different system sizes as a function of  $\lambda$  for the LMG model coupled to a central qubit ( $\gamma = 0$ ). The normalized  $\chi$  for various system sizes collapse to a single curve.

order in the  $1/N$  expansion of the HP transformation. To obtain more accurate results near the critical point, one have to go to higher order terms in the  $1/N$  expansion of HP transformation [17] or through the analysis of the Majorana polynomial roots [18]. In this report, our focus is on the scaling behavior of  $\chi$  within the same phase of the model. The analytical analysis presented so far remains valid as long as one stays in the same phase.

Fig. 6 shows a plot of  $\chi$  obtained from exact diagonalization as a function of  $\lambda$  for the case of  $\gamma = 0.5$ .  $\chi$  shows different scaling behavior on two sides of  $\lambda = 1$ . This is the quantum critical point of the LMG model. For  $\lambda > 1$ , the system is in the polarized phase and spins are polarized along the  $z$ -direction. In this phase,  $\chi$  for different system sizes collapse to a single curve indicating that  $\chi \sim N^0$ . For  $\lambda < 1$ , the model is in the symmetry-broken phase. The spin-spin interaction in the model in the  $xy$  plane dominates. The normalized  $\chi$  for different size collapse into a single curve and one has  $\chi \sim N$ . These results are consistent with the scaling analysis using the analytical expression of  $\chi$  as shown in Eq. (38) and Eq. (40), respectively.

To interpret the results obtained, we argue that in order to observe the QZE in the symmetry broken phase, the number of measurements  $Q$  has to be of comparable order of  $N$ . In a thermodynamic system, this condition is hardly realized. However, in the polarized phase where  $\chi$  is independent of the system size, the QZE is much more easier to be observed in comparing to that in the symmetry broken phase. Physically, this may be understood by the fact that in the case where  $\lambda > 1$ , the ground state of the model is given by the configuration in which spins are already fully polarized along the external field.

Moreover, from Fig. 6, we also see that  $\chi$  shows some abnormal behavior at the quantum critical point of the LMG model. Fig. 7 shows a plot of the first derivative of

the normalized  $\chi$  with respect to  $\lambda$  near the vicinity of the critical point.  $d(\chi/N)/d\lambda$  exhibits a minimum near  $\lambda = 1$  and this minimum's amplitude increases as the system size increases. From the inset of the figure, one finds  $d(\chi/N)/d\lambda \sim N^{0.324 \pm 0.001}$ . In the thermodynamic limit where  $N \rightarrow \infty$ ,  $d(\chi/N)/d\lambda$  is expected to be divergent at the critical point.

Fig. 8 and 9 shows the numerical exact diagonalization result of  $\chi$  and  $d(\chi/N)/d\lambda$  as a function of  $\lambda$  respectively for the case of  $\gamma = 0$ . The scaling behavior of  $\chi$  obtained here is the same as the case for  $\gamma = 0.5$ . From the inset of Fig. 9, we also have  $d(\chi/N)/d\lambda \sim N^{0.328 \pm 0.001}$ , which is consistent with the case for  $\gamma = 0.5$  up to two digits.

## V. SUMMARY

In this report, we have investigated the QZE from the viewpoint of condensed matter physics. We have obtained the scaling behavior of  $\chi$  in two analytically solvable systems, namely the one-dimensional transverse-field Ising model and the LMG model. We have found that in the Ising model, the frequency of the projective measurement should be of comparable order to that of

the system sizes in order to observe the QZE, and similar conclusion is obtained for the case of the symmetry broken phase in the LMG model; however for the polarized phase of the LMG model, the QZE can be easily observed via frequent measurements. Since we know that the size of the system in the thermodynamic limit is of order  $10^{23}$ , in reality it is almost impossible to have such a high frequency of projective measurement by the current technology. In this sense, we can safely argue that under certain circumstances, the QZE may break down in the thermodynamic limit.

Furthermore, we also highlight the abnormal behavior of  $\chi$  as a function of the external driving parameter across the quantum critical point of the Ising model and the LMG model. The possibility of detecting QPT by QZE is raised and further exploration would be of interest.

## VI. ACKNOWLEDGEMENT

This work is supported by the Earmarked Grant Research from the Research Grants Council of HKSAR, China (Project No. HKUST3/CRF/09).

- 
- [1] B. Misra and E. C. G. Sudarshan, *J. Math. Phys.* **18**, 765 (1977).
  - [2] C. B. Chiu, E. C. G. Sudarshan, and B. Misra, *Phys. Rev. D* **16**, 520 (1977).
  - [3] G. C. Ghirardi, C. Omero, T. Weber, and A. Rimini, *Nuovo Cimento* **52A**, 421 (1979).
  - [4] A. Peres, *Am. J. Phys.* **48**, 931 (1980).
  - [5] K. Kraus, *Found. Phys.* **11**, 547 (1981).
  - [6] E. Joos, *Phys. Rev. D* **29**, 1626 (1984).
  - [7] D. Home and M. A. B. Whitaker, *J. Phys. A* **19**, 1847 (1986).
  - [8] J. Dziarmaga, *Adv. Phys.* **59**, 1063 (2010).
  - [9] W. H. Zurek, U. Dorner, and P. Zoller, *Phys. Rev. Lett.* **95**, 105701 (2005).
  - [10] J. Dziarmaga, *Phys. Rev. Lett.* **95**, 245701 (2005).
  - [11] L. Fonda, G. C. Ghirardi, A. Rimini, and T. Weber, *Nuov. Cim.* **15A**, 689 (1973).
  - [12] A. Degasperis, L. Fonda, and G. C. Ghirardi, *Nuov. Cim.* **21A**, 471 (1974).
  - [13] W. M. Itano, D. J. Heinzen, J. J. Bollinger, and D. J. Wineland, *Phys. Rev. A* **41**, 2295 (1990).
  - [14] J. F. Zhang *et al.*, *Phys. Rev. A* **79**, 012305 (2009).
  - [15] S. Sachdev, *Quantum Phase transition* (Cambridge University Press, Cambridge, England, 1999).
  - [16] H. T. Quan, Z. Song, X. F. Liu, P. Zanardi, and C.P. Sun, *Phys. Rev. Lett.* **96**, 140604 (2006).
  - [17] S. Dusuel, and J. Vidal, *Phys. Rev. B* **71**, 224420 (2005).
  - [18] P. Ribeiro, J. Vidal and R. Mosseri, *Phys. Rev. Lett.* **99**, 050402 (2007); P. Ribeiro, J. Vidal and R. Mosseri, *Phys. Rev. E* **78**, 021106 (2008).